

The measurement of pH in saline and hypersaline media at sub-zero temperatures:

Papadimitriou, Efsthios; Loucaides, Socratis; Rerolle, Victoire; Achtberberg, Eric P.; Dickson, Andrew G.; Moowlem, Matthew; Kennedy, Hilary

Marine Chemistry

DOI:

[10.1016/j.marchem.2016.06.002](https://doi.org/10.1016/j.marchem.2016.06.002)

Published: 20/08/2016

Peer reviewed version

[Cyswllt i'r cyhoeddiad / Link to publication](#)

Dyfyniad o'r fersiwn a gyhoeddwyd / Citation for published version (APA):

Papadimitriou, E., Loucaides, S., Rerolle, V., Achtberberg, E. P., Dickson, A. G., Moowlem, M., & Kennedy, H. (2016). The measurement of pH in saline and hypersaline media at sub-zero temperatures: Characterization of Tris buffers. *Marine Chemistry*, 184(August), 11-20.
<https://doi.org/10.1016/j.marchem.2016.06.002>

Hawliau Cyffredinol / General rights

Copyright and moral rights for the publications made accessible in the public portal are retained by the authors and/or other copyright owners and it is a condition of accessing publications that users recognise and abide by the legal requirements associated with these rights.

- Users may download and print one copy of any publication from the public portal for the purpose of private study or research.
- You may not further distribute the material or use it for any profit-making activity or commercial gain
- You may freely distribute the URL identifying the publication in the public portal ?

Take down policy

If you believe that this document breaches copyright please contact us providing details, and we will remove access to the work immediately and investigate your claim.

1 **The measurement of pH in saline and hypersaline media at sub-zero temperatures:**
2 **Characterization of Tris buffers**

3

4 Stathys Papadimitriou^{1,*}, Socratis Loucaides², Victoire Rérolle^{2,3}, Eric P. Achterberg^{4,5},
5 Andrew G. Dickson⁶, Matthew Mowlem², Hilary Kennedy¹

6

7 ¹Ocean Sciences, College of Natural Sciences, Bangor University, Menai Bridge, LL59 5AB,
8 UK

9 ²National Oceanography Centre, Southampton, SO14 3ZH, UK

10 ³Sorbonne Universités (UPMC, Univ Paris 06)-CNRS-IRD-MNHN, LOCEAN Laboratory,
11 75005, Paris, France

12 ⁴University of Southampton, National Oceanography Centre, Southampton, SO14 3ZH, UK

13 ⁵GEOMAR, Helmholtz Centre for Ocean Research, 24148 Kiel, Germany

14 ⁶Marine Physical Laboratory, Scripps Institution of Oceanography, University of California,
15 San Diego, 9500 Gilman Drive, La Jolla, CA 92093-0244, USA

16

17 *corresponding author, e-mail: s.papadimitriou@bangor.ac.uk

18 Revised manuscript MARCHE_D1600001 Round 2

19

20 **Abstract**

21 The pH on the total proton scale of the Tris-HCl buffer system (pH_{Tris}) was characterized
22 rigorously with the electrochemical Harned cell in salinity (S) 35 synthetic seawater and S =
23 45 – 100 synthetic seawater-derived brines at 25 and 0°C, as well as at the freezing point of the
24 synthetic solutions (–1.93°C at S = 35 to –6°C at S = 100). The electrochemical characterization
25 of the common equimolar Tris buffer [$R_{\text{Tris}} = m_{\text{Tris}}/m_{\text{Tris-H}^+} = 1.0$, with $m_{\text{Tris}} = m_{\text{Tris-H}^+} = 0.04$
26 mol $\text{kg}_{\text{H}_2\text{O}}^{-1}$ = molality of the conjugate acid-base pair of 2-amino-2-hydroxymethyl-1,3-
27 propanediol (Tris)] yielded pH_{Tris} values which increased with increasing salinity and
28 decreasing temperature. The electrochemical characterization of a non-equimolar Tris buffer
29 variant ($R_{\text{Tris}} = 0.5$, with $m_{\text{Tris}} = 0.02$ mol $\text{kg}_{\text{H}_2\text{O}}^{-1}$ and $m_{\text{Tris-H}^+} = 0.04$ mol $\text{kg}_{\text{H}_2\text{O}}^{-1}$) yielded pH_{Tris}
30 values that were consistently less alkaline by 0.3 pH unit than those of the equimolar Tris
31 buffer. This is in agreement with the values derived from the stoichiometric equilibrium of the
32 Tris-H⁺ dissociation reaction, described by the Henderson – Hasselbalch equation, $\text{pH}_{\text{Tris}} =$
33 $\text{pK}_{\text{Tris}}^* + \log R_{\text{Tris}}$, with $\text{pK}_{\text{Tris}}^*$ = stoichiometric equilibrium dissociation constant of Tris-H⁺,
34 equivalent to equimolar pH_{Tris} . This consistency allows reliable use of other R_{Tris} variants of
35 the Tris-HCl buffer system within the experimental conditions reported here. The results of
36 this study will facilitate the pH measurement in saline and hypersaline systems at below-zero
37 temperatures, such as sea ice brines.

38

39 **Keywords**

40 Calibration, standards, pH, traceability, sea ice, brine, low temperature

41

42 **Introduction**

43 High latitude oceans contribute disproportionately to the CO₂ uptake from the atmosphere
44 (Bates and Mathis, 2009; Takahashi et al., 2002), but these estimates are based on data
45 generated by sampling ice-free parts of the polar oceans. A complete picture of the polar CO₂
46 budget must include the role of the seasonal and perennial sea ice in CO₂ cycling and air-sea
47 exchange in these regions. Recent research has demonstrated that brine pockets in sea ice are
48 sites of physical and biogeochemical processing that render sea ice an environment of active
49 carbon cycling (Arrigo et al., 1997; Dieckmann et al., 2008; Gleitz et al., 1995; Miller et al.,
50 2011a, 2011b; Munro et al., 2010; Papadimitriou et al., 2012; Rysgaard et al., 2011; Rysgaard
51 et al., 2007). Processes, such as primary and secondary production (Arrigo et al., 1997;
52 Deming, 2010), mineral authigenesis, including CaCO₃ in the form of ikaite (Dieckmann et al.,
53 2010; Dieckmann et al., 2008; Rysgaard et al., 2013), gas exchange (Miller et al., 2011a, 2011b;
54 Papadimitriou et al., 2012; Papadimitriou et al., 2004), and brine drainage (Notz and Worster,
55 2009) have dynamic seasonal cycles in sea ice and affect the carbonate system at the ocean-air
56 interface in high latitudes (Bates and Mathis, 2009; Bates et al., 2006; Chierici and Fransson,
57 2009; Dieckmann et al., 2008; Fischer et al., 2013; Miller et al., 2011b; Papadimitriou et al.,
58 2014; Papadimitriou et al., 2013; Rysgaard et al., 2012; Takahashi et al., 2002; Yamamoto-
59 Kawai et al., 2011; Yamamoto-Kawai et al., 2009). However, in comparison with the current
60 advancement of our knowledge on ice-free waters of the high latitude oceans, the study of the
61 carbonate system in sea ice has been patchy, not least because of logistical and physical-
62 chemical complexities (Miller et al., 2015).

63 Sea ice is a porous medium of mostly pure ice with a small percentage by volume of
64 brine and gas pockets (Cox and Weeks, 1983). The chemical composition of the liquid and gas
65 phases of sea ice results from the physical-chemical changes attendant on seawater freezing,
66 its dissolved salt and gas expulsion from the pure ice matrix, and their entrapment and physical
67 concentration in pockets within (Cox and Weeks, 1983). Thus, sea ice brines exhibit a much
68 wider range of salinity (*S*) and temperature (*t*) within short temporal and spatial scales than the
69 underlying and ice-free oceanic waters. The temperature of sea ice ranges from the freezing
70 point of seawater at the ice-water interface [$t_{fr} = -1.93^{\circ}\text{C}$ at 1 atm total pressure and $S = 35$;
71 UNESCO (1983)] to temperatures as low as -16°C , or even lower during winter, in the coldest
72 upper parts of ice floes in contact with the atmosphere (Miller et al., 2011a, 2011b)
73 accommodating hypersaline ($S \gg 35$) brines of an equivalent freezing point. For example, at
74 -6°C , about 66% of the water is present as ice and the residual brine has a salinity of 100. The
75 temperature range where in situ investigation of the carbonate system in sea ice would be most

76 beneficial is between the freezing point of seawater and the temperature at which the sea ice
77 becomes impermeable to liquid transport and material exchange with the underlying ocean.
78 This occurs when the brine volume becomes less than 5%, which occurs at -5°C when bulk
79 sea ice $S = 5$ (Golden et al., 1998).

80 For the investigation of the carbonate system under such S - t conditions as found in sea
81 ice, total alkalinity (TA), total dissolved inorganic carbon (DIC), and dissolved CO_2 (as gas
82 fugacity, $f\text{CO}_2$) measurements are possible using current methodologies and instrumentation
83 (Miller et al., 2015) but not the measurement of pH, which is only possible thus far at above-
84 zero temperatures and salinities up to 40. An estimate of the pH at the sub-zero temperatures
85 and high salinities of sea ice brines can be computed from the solution of the thermodynamic
86 model that describes the oceanic carbonate system using measurements of TA and DIC as input
87 parameters (Brown et al., 2014; Delille et al., 2007; Gleitz et al., 1995; Papadimitriou et al.,
88 2007; Papadimitriou et al., 2004). This requires knowledge of the dissociation constants of
89 carbonic and boric acids at the salinity and temperature ranges of sea ice. Empirical data for
90 these constants, however, do not exist for $t < 0^{\circ}\text{C}$ and $S > 50$ in natural solutions (Dickson,
91 1990a; Millero et al., 2006). The required extrapolation to lower temperatures and higher
92 salinities of the non-linear S - t functions that describe the existing empirical data set can result
93 in sizeable errors in these computations (Brown et al., 2014). With this caveat in mind, the
94 estimated in situ pH in sea ice brines has been reported to range between 7 and 10 (Delille et
95 al., 2007; Gleitz et al., 1995; Miller et al., 2011a; Papadimitriou et al., 2007). Finally, the use
96 of the traditional pH measurement techniques (potentiometry, spectrophotometry) at sub-zero
97 temperatures and high salinities is challenging because of untested electrochemical behaviour
98 of glass electrodes used in potentiometry, lack of experimental data for the optical parameters
99 and dissociation constants of pH indicator dyes used in spectrophotometry, and lack of suitable
100 calibration buffers compounding the uncertainties of both potentiometric and
101 spectrophotometric methods at sub-zero temperatures and hypersaline conditions. The range
102 of environmental conditions for which saline pH buffers have been characterized is $0 - 40^{\circ}\text{C}$
103 and $S = 20 - 40$ for the 2-amino-2-hydroxymethyl-1,3-propanediol (Tris) compound in
104 synthetic seawater (DeValls and Dickson, 1998), as well as $5 - 45^{\circ}\text{C}$ and $S = 35$ for 2-amino-
105 2-methyl-1,3-propanediol (Bis), tetrahydro-1,4-isoxazine (Morpholine), and 2-amino-pyridine
106 (Aminopyridine) (Millero et al., 1993), all on the total proton scale. Similarly, pH indicator
107 dyes have typically been characterized at above-zero temperatures and $S < 40$ conditions on
108 the total and free proton scales (e.g., Liu et al., 2011; Robert-Baldo et al., 1985), with a further
109 extension of the dye data set on the free proton scale in NaCl solutions by Millero et al. (2009)

110 to the full ionic strength spectrum up to NaCl saturation ($0.03 < I < 5.50$ molal) at above-zero
111 temperatures. Overall, there is currently no validated method for measuring pH at sub-zero
112 temperatures or, especially, in the coupled sub-zero temperature and high salinity of sea ice
113 brines, or at any temperature for $S > 40$ in multi-electrolyte media.

114 The aim of this work was to enable reliable measurement of pH in saline and hypersaline
115 media at sub-zero temperatures. To this end, we determined the pH of Tris buffer solutions in
116 corresponding salinity and temperature conditions. For this task, we extended the standard
117 electrochemical protocol for pH buffer characterization to international standards in the Harned
118 (hydrogen gas/silver/silver chloride) cell (Bates, 1973) described in the oceanographic pH
119 literature (Campbell et al., 1993; DelValls and Dickson, 1998; Dickson, 1990a, 1990b; Millero
120 et al., 1993). The electrochemical characterization of pH buffers is an essential first step in the
121 characterization of pH indicator dyes for use in the spectrophotometric pH determination. The
122 characterization of the pH indicator dye *meta*-Cresol Purple (mCP) with a microfluidic flow
123 spectrophotometric cell in the same temperature and salinity ranges will be reported in a
124 companion paper. The results relayed here will therefore promote the acquisition of high
125 quality in situ measurements of pH in polar waters and sea ice brines, and will improve the
126 confidence in future investigations of this parameter of the carbonate system in these
127 environments.

128

129 **Methods**

130 The pH of equimolal and non-equimolal Tris buffers (pH_{Tris}) in synthetic seawater and
131 brines was determined with the electrochemical Harned cell (Bates, 1973), the only rigorous
132 method available for the characterization of primary buffer solutions (IUPAC, 2002). The
133 characterization was conducted in the Marine Physical Laboratory, Scripps Institution of
134 Oceanography, University of California, San Diego, USA. The determination of the pH_{Tris}
135 requires the determination of the standard potential of the Harned cell from e.m.f.
136 measurements with pure HCl solutions, HCl solutions prepared in the synthetic medium, and
137 in HCl solutions in the synthetic medium with Tris. Details of the all-glass type Harned cell,
138 and the silver-silver chloride and hydrogen electrodes used in this study can be found in
139 DelValls and Dickson (1998). The solutions were analysed in duplicate or triplicate at each
140 HCl molality in the Harned cells in a thermostated water-glycol bath. The bath temperature
141 was controlled to 0.01°C and all e.m.f. measurements were corrected to 1 atm hydrogen gas
142 fugacity (DelValls and Dickson, 1998). We characterized the Tris-HCl buffer in the standard

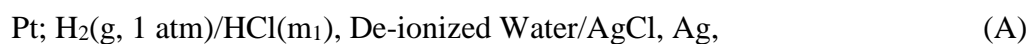
143 equimolal Tris/Tris-H⁺ composition (0.08 mol kg_{H₂O}⁻¹ Tris, 0.04 mol kg_{H₂O}⁻¹ HCl) and in a less
 144 alkaline non-equimolal Tris/Tris-H⁺ composition (0.06 mol kg_{H₂O}⁻¹ Tris, 0.04 mol kg_{H₂O}⁻¹ HCl)
 145 in synthetic high ionic strength multi-electrolyte solutions matching the ionic ratios of standard
 146 seawater and seawater-derived brines. The synthetic solutions were prepared gravimetrically
 147 using the recipe in Table 1, which was based on that of standard seawater (S = 35) in DelValls
 148 and Dickson (1998). All synthetic solutions were prepared with purified salts, to maximize
 149 stability in the electrochemical response of the Harned cell. All salts (NaCl, Na₂SO₄, KCl,
 150 CaCl₂, MgCl₂) were twice re-crystallized from reagent grade salts, air-dried, annealed at
 151 200°C, and (except for CaCl₂ and MgCl₂) were heated to 500°C (10 hrs) (Dickson, 1990a;
 152 Millero et al., 1993). The CaCl₂ and MgCl₂ salts were used to prepare approximately 1 mol
 153 kg_{solution}⁻¹ Ca²⁺ and Mg²⁺ working stock solutions, which were used for the preparation of the
 154 synthetic media. The concentration of Ca²⁺ and Mg²⁺ in these stock solutions was determined
 155 gravimetrically with a relative standard deviation better than 0.1% by Mohr titration with 0.3
 156 mol kg_{solution}⁻¹ AgNO₃, itself standardized similarly against purified NaCl and KCl (Dickson,
 157 1990a; Millero et al., 1993). The working stock HCl solution (approximately 1 mol kg_{solution}⁻¹)
 158 was prepared gravimetrically with de-ionized water from double-distilled 6 M HCl solution.
 159 The concentration of these HCl solutions was determined by coulometry with a relative
 160 standard deviation better than 0.001%. It is standard practice to adjust the e.m.f. measurements
 161 in synthetic salt solutions so that their standard potential corresponds to that of Bates and Bower
 162 (1954). The adjustment factor is determined from e.m.f. measurements in dilute HCl solutions
 163 as described in the next section.

164

165 **The standard potential of pure HCl solutions**

166 The standard potential ($E_o = \text{e.m.f. at infinite proton dilution}$) of the cell

167



169

169 was determined regularly to ensure conformity with the measurements by Bates and Bower
 170 (1954). The E_o of cell (A) was derived by solving the Nernst equation as $E_o = E + 2k \ln(\gamma_{\pm\text{HCl}} m_{\text{HCl}})$, where E = measured e.m.f., $\gamma_{\pm\text{HCl}}$ = mean activity coefficient of HCl, $m_{\text{HCl}} = m_1$ in cell
 171 (A), and $k = RT/F$, with R = gas constant = 8.31451 J mol⁻¹ K⁻¹, T = absolute temperature (in
 172 K), and F = Faraday constant = 96485.31 C mol⁻¹. The $\gamma_{\pm\text{HCl}}$ was computed as a function of
 173

174 ionic strength and temperature using the Pitzer parameterization. In the Pitzer formalism
 175 (Pitzer, 1973), the mean activity coefficient of HCl as an 1–1 electrolyte is calculated as $\ln\gamma_{\pm\text{HCl}}$
 176 $= f' + m_{\text{HCl}} B_{\text{HCl}}^{(\gamma)} + m_{\text{HCl}}^2 C_{\text{HCl}}^{(\gamma)}$, with $f' = -A^\phi \{ [\Gamma^{0.5}/(1 + b\Gamma^{0.5})] + (2/b) \ln(1 + b\Gamma^{0.5}) \}$, $B_{\text{HCl}}^{(\gamma)} = 2$
 177 $\beta_{\text{HCl}}^{(o)} + [2\beta_{\text{HCl}}^{(1)}/(\alpha^2 I)] [1 - (1 + \alpha I^{0.5} - 0.5\alpha^2 I) e^{-\alpha I^{0.5}}]$, and $C_{\text{HCl}}^{(\gamma)} = 1.5 C_{\text{HCl}}^{(\phi)}$, where $\alpha = 2.0$ and
 178 $b = 1.2$, while molality (m) and ionic strength (I) are in $\text{mol kg}_{\text{H}_2\text{O}}^{-1}$. The Pitzer coefficients, A^ϕ ,
 179 $\beta_{\text{HCl}}^{(o)}$, $\beta_{\text{HCl}}^{(1)}$, and $C_{\text{HCl}}^{(\phi)}$, were all computed from the temperature functions in Millero (2009).
 180 At the HCl molality and ionic strength (both $0.010 \text{ mol kg}_{\text{H}_2\text{O}}^{-1}$) and temperatures used most
 181 frequently in this study for the E_o determination, $\gamma_{\pm\text{HCl}} = 0.9046$ at 25°C and 0.9083 at 0°C .

182 The E_o determined in this study as described above (E_o^{measured}) and by Bates and Bower
 183 (1954) (E_o^{BB}) as computed from the temperature function in Dickson (1990b) yielded the offset
 184 $\Delta E_o^{\text{BB}} = E_o^{\text{measured}} - E_o^{\text{BB}}$. At the temperatures that E_o^{measured} was determined in this study, E_o^{BB}
 185 is 0.22240 V at 25°C , 0.23408 V at 5°C , and 0.23659 V at 0°C . To determine ΔE_o^{BB} , cell (A)
 186 was run on several occasions in parallel with the cells with synthetic saline and hypersaline
 187 media described in the next two sections. On average, $\Delta E_o^{\text{BB}} = -0.00012 \pm 0.00024 \text{ V}$ ($n = 39$)
 188 with $m_{\text{HCl}} = 0.010 \text{ mol kg}_{\text{H}_2\text{O}}^{-1}$ and $\Delta E_o^{\text{BB}} = -0.00052 \pm 0.00016 \text{ V}$ ($n = 4$) with $m_{\text{HCl}} = 0.005$
 189 $\text{mol kg}_{\text{H}_2\text{O}}^{-1}$ in cell (A) at $0, 5, \text{ and } 25^\circ\text{C}$ during Harned cell runs with $S = 35$ synthetic seawater,
 190 while $\Delta E_o^{\text{BB}} = 0.00000 \pm 0.00005 \text{ V}$ ($n = 37$) with $m_{\text{HCl}} = 0.010 \text{ mol kg}_{\text{H}_2\text{O}}^{-1}$ in cell (A) at 0 and
 191 25°C during Harned cell runs with $S = 45 - 70$ synthetic brines, and $\Delta E_o^{\text{BB}} = +0.00002 \pm$
 192 0.00005 V ($n = 17$) with $m_{\text{HCl}} = 0.010 \text{ mol kg}_{\text{H}_2\text{O}}^{-1}$ in cell (A) at 0 and 25°C during Harned cell
 193 runs with $S = 85 - 100$ synthetic brines. To adjust the e.m.f. measurements in synthetic salt
 194 solutions so that their standard potential corresponds to that of Bates and Bower (1954), the
 195 average ΔE_o^{BB} per group of saline and hypersaline Harned cell runs was subtracted from all
 196 e.m.f. measurements in these media. The adjusted e.m.f. measurements and the ΔE_o^{BB} values
 197 used for their adjustment are reported in Table S1 in Supplementary Information for cells (B)
 198 and (C) and in Table 3 for cells (D) and (E); these cells are described in the next two sections.

199

200 **The apparent standard potential of the Harned cell with synthetic seawater ($S = 35$) and**
 201 **synthetic brine ($S > 35$)**

202 The e.m.f. measurements in the cells

203

Pt; H₂(g, 1 atm)/ HCl(m₁), Synthetic Seawater (S = 35)/ AgCl, Ag (B)

Pt; H₂(g, 1 atm)/ HCl(m₁), Synthetic Brine (S > 35)/ AgCl, Ag (C)

204

205 were used to determine their apparent standard potential (E_o^*) in the presence of sulphate in the
 206 synthetic solutions of this study. Sulphate ions react with protons to form bisulphate ($SO_4^{2-} +$
 207 $H^+ = HSO_4^-$), with a stoichiometric dissociation constant $K_{HSO_4^-} = m_{H^+} m_{SO_4^{2-}} / m_{HSO_4^-}$. In this
 208 case, instead of the free proton scale (m_{H^+}), the total proton scale has been used previously,
 209 defined as $m_{H^+}^T = m_{H^+} + m_{HSO_4^-} = m_{H^+} (1 + m_{SO_4^{2-}} / K_{HSO_4^-})$, with $m_{H^+}^T = m_{HCl} = m_1$ in cells (B)
 210 and (C) above (Campbell et al., 1993; Dickson, 1990b). Thermodynamically rigorous, the total
 211 proton scale is suitable for the determination of acidity constants (Dickson, 1990b) and, as per
 212 objective of this study, is also used here to define and determine the pH of Tris buffers in
 213 keeping with previous studies (Campbell et al., 1993; DelValls and Dickson, 1998).
 214 Conversion to the free proton scale requires knowledge of $K_{HSO_4^-}$, which is not available at
 215 below-zero temperatures. It is beyond the scope of this study to determine $K_{HSO_4^-}$ because it is
 216 not needed to determine acidity constants in the total proton scale; as outlined below, this
 217 parameter is incorporated in the determined E_o^* term of the Nernst equation for cells (B) and
 218 (C).

219 The E_o^* is given by re-arrangement of the Nernst equation as $E_o^* = E_o - 2 k \ln \gamma_{\pm HCl} + k$
 220 $\ln(1 + m_{SO_4^{2-}} / K_{HSO_4^-}) = E + k \ln(m_{HCl} m_{Cl^-})$ (Campbell et al., 1993; Dickson, 1990b; Millero
 221 et al., 1993). Here, E_o , k , and $\gamma_{\pm HCl}$ are as explained in the previous section, $K_{HSO_4^-}$ and m_{HCl} as
 222 above, $m_{SO_4^{2-}}$ = total sulphate molality, m_{Cl^-} = total chloride molality, and E = measured e.m.f.
 223 in cells (B) and (C) above adjusted by ΔE_o^{BB} . The value of $E_o^* = E_o - 2 k \ln \gamma_{\pm HCl} + k \ln(1 +$
 224 $m_{SO_4^{2-}} / K_{HSO_4^-})$ is determined at each temperature and salinity at $m_{HCl} \rightarrow 0$, the standard state
 225 of infinite dilution in the pure medium, as the intercept of the quadratic function, $E' = E + k$
 226 $\ln(m_{HCl} m_{Cl^-}) = a + b m_{HCl} + c m_{HCl}^2$, with $E_o^* = a$ (Campbell et al., 1993; Dickson, 1990b). The
 227 adjusted e.m.f. measurements in synthetic solutions of several different HCl molalities ($n = 5$
 228 – 6) at each salinity and temperature (given in Table S1 in Supplementary Information) were
 229 used to obtain E' . The experimental E' values were fitted to a quadratic function of m_{HCl} with

230 least-squares regression in Excel (shown for $S = 35$ and 45 in Fig. 1) to obtain E_o^* and its
 231 standard error (equivalent to that of the intercept of the quadratic fit), which are both given in
 232 Table 2. The adjusted squared correlation coefficient of the quadratic fits ranged from 0.9421
 233 to 0.9997 ($p < 0.00001$) and the standard error of the fits from 0.00001 to 0.00011 V. Cell (B)
 234 was investigated with $m_{\text{HCl}} = 0.005 - 0.040 \text{ mol kg}_{\text{H}_2\text{O}}^{-1}$ at 25, 0, -0.6 , -1.2 , and -1.7°C , the
 235 last temperature close to the freezing point of surface oceanic water [-1.93°C , $S = 35$; UNESCO
 236 (1983)]. Cell (C) was investigated with $m_{\text{HCl}} = 0.010 - 0.050 \text{ mol kg}_{\text{H}_2\text{O}}^{-1}$ for $S = 45 - 100$ at
 237 25 and 0°C , as well as the freezing point of the synthetic brine (-2.5 to -6.0°C). The freezing
 238 point of the synthetic brines was computed from the inversion of the empirical absolute
 239 salinity-temperature (S_A - t) relationship of sea ice brines at ice-brine equilibrium, $S_A = 1000 (1$
 240 $- 54.11/t)^{-1}$ (Assur, 1958).

241

242 **Determination of the pH_{Tris} in synthetic seawater ($S = 35$) and synthetic brines ($S > 35$)**

243 The values of E_o^* in cells (B) and (C) (Table 2) were combined with e.m.f. measurements
 244 in cells (D) and (E) below, adjusted by ΔE_o^{BB} as described in the previous sections, to
 245 determine at each salinity and temperature the value of pH_{Tris} in $\text{mol kg}_{\text{solution}}^{-1}$ as $\text{pH}_{\text{Tris}} = (E$
 246 $- E_o^*) / (k \ln 10) + \log m_{\text{Cl}^-} - \log(1 - 0.00106 S)$ (DelValls and Dickson, 1998) (Table 3). In this
 247 equation, $\ln 10$ is the conversion factor between logarithmic scales and all other parameters are
 248 as before, while the last term on the right side of this equation serves to convert the pH value
 249 from $\text{mol kg}_{\text{H}_2\text{O}}^{-1}$ to $\text{mol kg}_{\text{solution}}^{-1}$.

250



251

252 With $[\text{Tris-H}^+] = m_1$ and $[\text{Tris}] = m_2 - m_1$ in cells (D) and (E) above, at stoichiometric
 253 equilibrium, the reaction, $\text{Tris} + \text{HCl} = \text{Tris-H}^+ + \text{Cl}^-$, leads to equimolar Tris and Tris-H^+
 254 molalities in cell solutions containing $m_1 = 0.04 \text{ mol kg}_{\text{H}_2\text{O}}^{-1}$ HCl and $m_2 = 0.08 \text{ mol kg}_{\text{H}_2\text{O}}^{-1}$
 255 Tris. Because the equimolar pH_{Tris} is alkaline at low temperatures ($\text{pH}_{\text{Tris}} \approx 9$), a less alkaline,
 256 non-equimolar Tris buffer was also characterized with the Harned cell protocol with $m_1 = 0.04$
 257 $\text{mol kg}_{\text{H}_2\text{O}}^{-1}$ and $m_2 = 0.06 \text{ mol kg}_{\text{H}_2\text{O}}^{-1}$, yielding a stoichiometric molality ratio, $R_{\text{Tris}} = m_{\text{Tris}} /$
 258 $m_{\text{Tris-H}^+} = 0.5$. To examine the internal consistency of the e.m.f. measurements in these non-

259 equimolal Tris-HCl buffers, their pH was also computed from the equimolal pH_{Tris} , when
260 available, and their R_{Tris} using the Henderson – Hasselbalch equation (Pratt, 2014), $\text{pH}_{\text{Tris}} =$
261 $\text{pK}_{\text{Tris}}^* + \log R_{\text{Tris}}$, which is derived from the stoichiometric equilibrium of the Tris-H^+
262 dissociation reaction (Millero, 2009), with $\text{pK}_{\text{Tris}}^*$ equivalent to the equimolal pH_{Tris} when R_{Tris}
263 $= 1$.

264 The E_o^* and pH_{Tris} data from this study alone and combined with relevant data at above-
265 zero temperatures from earlier studies were fitted to non-linear equations of temperature and
266 salinity or ionic strength using the Regression function in the Data Analysis Tool of Excel. The
267 fitted coefficients of these equations, along with the adjusted squared correlation coefficient
268 (r^2) and the standard error of the fit (σ_{fit}), as well as the number of fitted observations (n), are
269 all reported from the Regression output in subsequent sections. Information about the standard
270 error of the individual fitted coefficients is reported in Tables S2 and S3 in Supplementary
271 Information.

272

273 **Results**

274 The focus of this study was the characterization of the pH of Tris buffers at below-zero
275 temperatures but e.m.f. measurements were also obtained at 25 and 0°C for evaluation relative
276 to the existing datasets at overlapping temperature and salinity ranges. We kept this protocol
277 throughout the experimental salinity range (35 – 100) and report the results at 25 and 0°C here
278 in order to provide data useful for occasions in sea ice studies when pH measurement at sub-
279 zero temperatures is not possible due to harsh field conditions and restrictions by equipment or
280 method.

281

282 **The standard potential of the Harned cell to the freezing point of synthetic seawater and** 283 **brines**

284 The E_o^* values at each experimental temperature and salinity along with their standard
285 error are given in Table 2 and are shown in Fig. 2. The e.m.f. measurements at $S = 35$ (Fig.
286 1a,b) were consistent with published data at 25 and 0°C (Campbell et al., 1993; Dickson,
287 1990b; Khoo et al., 1977), while those made at $S = 45$ (Fig. 1c,d) were consistent with the
288 values in Khoo et al. (1977) at 25°C. The current E_o^* values at 25 and 0°C and $S = 35$ and 45
289 were different by less than +0.00030 V from previous determinations in these conditions
290 (Campbell et al. 1993; Dickson 1990b). No other direct comparison is possible as the remainder
291 of the current data extend beyond the temperature minimum and salinity maximum of the

292 previous data sets. An indirect comparison can be made using the extrapolation of the ionic
 293 strength and temperature function of E_o^* in Dickson (1990b) and in Campbell et al. (1993).
 294 This will also allow a direct evaluation of the extrapolation as practiced by necessity so far by
 295 sea ice scientists.

296 The current E_o^* values at below-zero temperatures and $S = 35$ were +0.00010 to
 297 +0.00020 V and +0.00060 V different from those predicted by extrapolation of the equations
 298 in Dickson (1990b) and Campbell et al. (1993), respectively (Table 2). These differences are
 299 equivalent to 0.002 – 0.011 pH unit for the Tris buffer in synthetic seawater. A revised non-
 300 linear function of temperature is given below for E_o^* in synthetic seawater ($S = 35$) from the
 301 regression fit to the combined past and current data from 55 to -1.7°C ($r^2 = 0.99995$, $p <$
 302 0.00001 , $n = 27$, $\sigma_{fit} = 0.00004$ V; the fitted residuals are shown in Fig. S1a in Supplementary
 303 Information), with E_o = the Bates and Bower (1954) standard potential of the Harned cell as
 304 fitted by Dickson (1990b) and T = temperature (in K):

$$E_o^* - E_o = 0.583228 - 1.5914057 \times 10^{-2} T + 2.5229012 \times 10^{-3} T \ln T - 1.12824 \times 10^{-6} T^2, \quad (1)$$

306
 307 The difference between the current E_o^* values in the synthetic brines ($S \geq 45$) and the
 308 extrapolated values from the existing equations (Table 2) ranged from +0.00020 to +0.00670
 309 V (equivalent to 0.003 – 0.118 pH unit), increasing with increasing salinity throughout the
 310 experimental temperature range (Fig. 2). The current measurements provide for a more
 311 accurate and reliable measurement of the pH in ice-brine systems. To facilitate this application,
 312 we combined the E_o^* value at the freezing point of seawater derived from eq. (1) above ($E_o^* =$
 313 0.25540 V at -1.93°C and $S = 35$ at 1 atm total pressure) with the values obtained at the
 314 different freezing points of $S \geq 45$ brines (Table 2) to obtain a best-fit temperature function of
 315 E_o^* applicable to thermally equilibrated sea ice brines. We found E_o^* to be best described (r^2
 316 $= 0.98906$, $p = 0.00005$, $n = 7$, $\sigma_{fit} = 0.00015$ V; the fitted residuals are shown in Fig. S1b in
 317 Supplementary Information) by a quadratic function of temperature (T , in K) at the freezing
 318 point of seawater and seawater-derived brines from -1.93 to -6.00°C ($S = 35 - 100$):

$$E_o^* = -11.632112 + 8.7319058 \times 10^{-2} T - 1.60345606 \times 10^{-4} T^2, \quad (2)$$

320

321 An extended equation is provided below for the computation of E_o^* by interpolation at
 322 any salinity and temperature outside the restricted conditions of equations (1) and (2) above
 323 but within the limits of the experimental range. The interpolation will be useful for the
 324 characterization of pH buffers (on the total proton scale) on such occasions. Although the
 325 current E_o^* data set is sparse as a function of temperature, it was combined with the data sets
 326 in Dickson (1990b) and Campbell et al. (1993) for an overall best fit ($r^2 = 0.99186$, $p < 0.00001$,
 327 $n = 133$, $\sigma_{fit} = 0.00008$ V) in the function format of the previous studies in ionic strength (I, in
 328 molality) and temperature (T, in K), with E_o from Dickson (1990b) as before:

329

$$\begin{aligned}
 E_o^* - E_o = & (0.8416344 - 2.0574375 \times 10^{-2} T + 3.1544753 \times 10^{-3} T \ln T - 2.6635 \times 10^{-8} T^2) I^{0.5} \\
 & + (-0.3356577 + 7.581873 \times 10^{-3} T - 1.1680967 \times 10^{-3} T \ln T) I \\
 & + (1.1146 \times 10^{-2} + 4.525 \times 10^{-5} T) I^{1.5} - 4.67174 \times 10^{-3} I^2, \quad (3)
 \end{aligned}$$

330

331 In the above equation, the ionic strength was calculated as a function of salinity as described
 332 in Table 1, while the fitted residuals are shown in Fig.3. Equation (3) is valid at temperatures
 333 (i) between 0 and 55°C for $I < 0.7225$ molal ($S < 35$), (ii) between the freezing point and 55°C
 334 for $0.7225 \text{ molal} \leq I \leq 0.9387 \text{ molal}$ ($35 \leq S \leq 45$), and (iii) between the freezing point and
 335 25°C for $0.9387 \text{ molal} < I \leq 2.2136 \text{ molal}$ ($45 < S \leq 100$). At 25°C and $I = 0.7225$ molal,
 336 equation (3) yields $E_o^* = 0.24627$ V, while at -6°C and $I = 2.2136$ molal, $E_o^* = 0.25145$ V (see
 337 Table 2 for observed values).

338

339 **The pH of Tris buffers to the freezing point of synthetic seawater and brines**

340 The pH values of the equimolal Tris buffer are listed in Table 3 and are shown in Fig. 4.
 341 The equimolal pH_{Tris} in synthetic seawater at 25°C and 0°C from the observed E_o^* (Table 2)
 342 and the e.m.f. measurements in cells (D) and (E) (Table 3) was within 0.002 pH unit from the
 343 values computed from the salinity and temperature function in DelValls and Dickson (1998)
 344 based on their experimental measurements at $S = 20 - 40$ and $0 - 45^\circ\text{C}$. The equimolal pH_{Tris}
 345 in synthetic seawater at sub-zero temperatures differed by 0.000 – 0.004 pH unit from the
 346 values obtained from the extrapolated DelValls and Dickson (1998) equation. The best-fit
 347 temperature (T, in K) function based on the combined current and previous data sets from 45°C
 348 to the freezing point of $S = 35$ seawater ($r^2 = 0.999997$, $p < 0.00001$, $n = 121$, $\sigma_{fit} = 0.001$ pH
 349 unit; the fitted residuals are shown in Fig. S2a in Supplementary Information) is given by the
 350 following equation:

351

$$\text{pH}_{\text{Tris}} (\text{equimolal}) = -322.08663 + 10570.47 \text{ T}^{-1} - 1.0408523 \times 10^{-1} \text{ T} + 57.17485 \ln \text{T}, \quad (4)$$

352

353 The equimolal pH_{Tris} in synthetic brines ($S \geq 45$) was determined up to $S = 70$. It was
 354 within 0.007 pH unit at $S = 45$ and 50 from the values predicted from the extrapolation of the
 355 DelValls and Dickson (1998) function but was lower than the extrapolated values by 0.009 –
 356 0.019 and 0.021 – 0.036 pH unit at $S = 60$ and 70, respectively, at all examined temperatures,
 357 suggesting increasingly unsuitable values from extrapolation at high salinities regardless of
 358 temperature (Fig. 4). Combining the value of the equimolal pH_{Tris} at the freezing point of $S =$
 359 35 seawater from eq. (4) above (equimolal $\text{pH}_{\text{Tris}} = 9.0039$ at -1.93°C) with the observations
 360 obtained at the different freezing points of $S \geq 45$ brines (Table 3), the equimolal pH_{Tris} at ice-
 361 brine thermal equilibrium was found to be best described ($r^2 = 0.99929$, $n = 9$, $p < 0.00001$, σ_{fit}
 362 $= 0.002$ pH unit; the fitted residuals are shown in Fig. S2b in Supplementary Information) to –
 363 4°C and $S = 70$ by the following function of temperature (T , in K):

364

$$\begin{aligned} \text{pH}_{\text{Tris}} (\text{equimolal}) = & -300435.6052 + 7240100.99 \text{ T}^{-1} - 99.5850583 \text{ T} \\ & + 53678.964954 \ln \text{T}, \end{aligned} \quad (5)$$

365

366 The non-equimolal $\text{pH}_{\text{R}_{\text{Tris}}=0.5}$ values are given in Table 3 and are shown in Fig. 4. On
 367 the occasions when both the equimolal and the non-equimolal buffers were measured ($35 \leq S$
 368 ≤ 70), the non-equimolal $\text{pH}_{\text{R}_{\text{Tris}}=0.5}$ values were within 0.001 pH unit from those determined
 369 from the Henderson – Hasselbalch equation described in the earlier section *Determination of*
 370 *the pH_{Tris} in synthetic seawater ($S = 35$) and synthetic brines ($S > 35$).* The $\text{pH}_{\text{R}_{\text{Tris}}=0.5}$ at the
 371 freezing point was determined for $50 \leq S \leq 100$ and $-6.0^\circ\text{C} \leq t \leq -2.8^\circ\text{C}$. The best-fit function
 372 of temperature (T , in K) for the non-equimolal $\text{pH}_{\text{R}_{\text{Tris}}=0.5}$ in the temperature and salinity
 373 conditions of thermally equilibrated seawater-derived brines is as follows ($r^2 = 0.99991$, $n =$
 374 13 , $p < 0.00001$, $\sigma_{\text{fit}} = 0.001$ pH unit; the fitted residuals are shown in Fig. S2c in Supplementary
 375 Information):

376

$$\begin{aligned} \text{pH}_{\text{R}_{\text{Tris}}=0.5} = & -725997.4416 + 17447191.73 \text{ T}^{-1} - 241.432111 \text{ T} \\ & + 129781.87456 \ln \text{T}, \end{aligned} \quad (6)$$

377

378 As mentioned at the beginning of the *Results* section, there can be occasions when the
 379 measurement of pH in cold media, such as sea ice brines, may not be possible at below-zero
 380 temperature. To provide interpolation power for these occasions, the data sets of the equimolal
 381 pH_{Tris} from this study and the study of DelValls and Dickson (1998) were combined to obtain
 382 a best fit in the format of the latter study, valid at temperatures (i) between 0 and 45°C for $S <$
 383 35, (ii) between the freezing point and 45°C for $35 \leq S < 45$, and (iii) between the freezing
 384 point and 25°C for $45 \leq S \leq 70$. The best fit equation in salinity (S) and temperature (T, in K)
 385 ($r^2 = 0.999995$, $n = 273$, $p < 0.00001$, $\sigma_{\text{fit}} = 0.001$ pH unit; the fitted residuals are shown in Fig.
 386 5a,c) is

$$\begin{aligned}
 \text{pH}_{\text{Tris}} (\text{equimolal}) = & 536.08338 - 54.732367 S + 0.8518518 S^2 \\
 & + (0.1675218 - 1.72224095 \times 10^{-2} S + 2.66720246 \times 10^{-4} S^2) T \\
 & + (-10873.5234 + 1369.56485 S - 21.34442 S^2) T^{-1} \\
 & + (-95.04342 + 9.7014355 S - 0.1509014 S^2) \ln T,
 \end{aligned} \tag{7}$$

388
 389 At 25°C and $S = 35$, equation (7) yields $\text{pH}_{\text{Tris}} (\text{equimolal}) = 8.094$, while at -4°C and S
 390 $= 70$, $\text{pH}_{\text{Tris}} (\text{equimolal}) = 9.191$ (see Table 3 for observed values). The equivalent overall fit
 391 on the current limited non-equimolal $\text{pH}_{\text{R-Tris}=0.5}$ data set yielded the following function of
 392 salinity and temperature (T, in K) at $50 \leq S \leq 100$ and from the freezing point of such brines to
 393 25°C ($r^2 = 0.99999$, $n = 41$, $p < 0.00001$, $\sigma_{\text{fit}} = 0.002$ pH unit; the fitted residuals are shown in
 394 Fig. 5b, d):

$$\begin{aligned}
 \text{pH}_{\text{R-Tris}=0.5} = & 144.4361 - 1.0809685 S + 6.023772 \times 10^{-3} S^2 \\
 & + (6.18411 \times 10^{-2} - 8.17397 \times 10^{-4} S + 4.27187 \times 10^{-6} S^2) T \\
 & + (-27.233738 + 0.2329236 S - 1.281138 \times 10^{-3} S^2) \ln T,
 \end{aligned} \tag{8}$$

396
 397 Using equation (8) above, the predicted $\text{pH}_{\text{R-Tris}=0.5} = 8.637$ at 0°C and $S = 35$, and
 398 $\text{pH}_{\text{R-Tris}=0.5} = 8.664$ at 0°C and $S = 45$. These values were within 0.004 pH unit from the
 399 measured values (Table 3), and so it is reliable to extend eq. (8) to these salinities.

400
 401 **Discussion**

402 The investigation of the carbonate system in oceanic waters and the determination of the
 403 potential for air-sea CO_2 exchange have intensified in an attempt to understand the implications

404 on global climate of the increase in the atmospheric CO₂ since the industrial revolution. The
405 required sampling and analytical protocols have been improved through continual method and
406 instrument development, allowing dense sampling in space and time for any pair of the 4
407 measurable parameters of the carbonate system (TA, DIC, pH, *f*CO₂) (DOE, 1994; Hales et al.,
408 2004; Liu et al., 2011). While the measurement of all 4 parameters is now routine in open ocean
409 waters (e.g., Millero et al., 2002), including polar waters (Bates and Mathis, 2009; Bates et al.,
410 2006), the same is not true for oceanic environments at sub-zero temperatures, such as sea ice.
411 At the salinity and temperature conditions in sea ice brines, the concentrations of TA and DIC,
412 as well as *f*CO₂ naturally cover large ranges controlled by the physical concentration of
413 seawater solutes during the freezing of seawater and further cooling of internal sea ice brines,
414 dilution of brine solutes by meltwater during sea ice melt, biological activity, CaCO₃
415 precipitation and dissolution, and CO₂ gas exchange (Delille et al., 2007; Dieckmann et al.,
416 2008; Gleitz et al., 1995; Miller et al., 2011a, 2011b; Munro et al., 2010; Papadimitriou et al.,
417 2012; Papadimitriou et al., 2007; Papadimitriou et al., 2004). By extension, large variations in
418 brine pH can also be expected in such environments, but there is only rudimentary knowledge
419 of pH changes in sea ice as direct determination of this parameter has been hampered by lack
420 of characterized calibration standards (buffers, indicator dyes) and unsuitable analytical set-
421 ups for the sub-zero temperatures and, in the case of internal sea ice brines, highly saline
422 conditions (*S* > 35).

423 Currently, the pH measurement protocols in sea ice and sub-zero temperature oceanic
424 waters, restricted by the temperature limitation of both buffers and technique, have only been
425 capable of pH measurements at (constant) above-zero temperature. For example, Delille et al.
426 (2007) used commercial glass electrodes and high salinity Tris and Aminopyridine buffers for
427 instrument calibration on samples returned to the laboratory and maintained at 1 – 3°C, and so
428 did Gleitz et al. (1995) at 20 – 22°C using NBS standard buffers. Miller et al. (2011a) used the
429 spectrophotometric technique with un-purified mCP as the pH-sensitive indicator dye at 25°C,
430 as did Hare et al. (2013) at 0°C. A technique based on the pH-sensitive fluorescence properties
431 of acridine and harmine has been developed and applied to fresh and salty ice surfaces, but
432 solely for monitoring rather than quantification of pH, due to lack of suitable characterization
433 and calibration of the fluorescence properties of these probes (Wren and Donaldson, 2012).

434 In this study, we electrochemically characterized the pH_T (total proton scale) of Tris-HCl
435 buffers using the Harned cell, the only rigorous method available for the task (IUPAC, 2002).
436 Use of these buffers can facilitate the calibration of the analytical pH instrumentation at the
437 experimental temperature and salinity ranges of this study. The pH_T of the Tris-HCl buffers

438 was increasingly alkaline with increasing salinity at constant temperature and with decreasing
439 temperature at constant salinity (Table 3; Fig. 4). The equimolal Tris buffer covered a pH_T
440 range from 8.09 at $S = 35$ and 25°C to 9.19 at the freezing point of an $S = 70$ synthetic brine ($-$
441 4°C) (Table 3). The pH_T of the non-equimolal ($R_{\text{Tris}} = 0.5$) Tris buffer ranged from 8.63 at $S =$
442 35 and 0°C to 9.06 at the freezing point of an $S = 100$ synthetic brine (-6°C) (Table 3) and was
443 0.3 pH units less alkaline than its equimolal counterpart (Fig. 4) as predicted using the
444 stoichiometric Tris-HCl equilibrium and the Henderson-Hasselbalch equation. On the strength
445 of this evidence and the study of Pratt (2014) in synthetic seawater, Tris-HCl buffers of varying
446 R_{Tris} and, hence, pH_T can be prepared if needed with the protocol outlined in *Methods*, and their
447 pH_T can be estimated reliably with the Henderson-Hasselbalch equation and the data presented
448 here for investigations within the temperature and salinity ranges of this study.

449 The pH_T ranges for the equimolal and non-equimolal ($R_{\text{Tris}} = 0.5$) Tris buffers covered
450 the alkaline spectrum of pH estimates at in-situ (below-zero) temperatures in sea ice. Delille et
451 al. (2007) reported pH_T values ranging from 8.4 to 9.4 in Antarctic fast ice brines ($S = 24 -$
452 89). In sackhole brines from the Weddell Sea, Antarctica, Papadimitriou et al. (2007)
453 determined a pH_{sws} (seawater proton scale) range of 8.4 to 8.8, while Gleitz et al. (1995)
454 reported a pH_{sws} range of 7.8 to 9.9. Hare et al. (2013) reported pH_T values between 7.1 and
455 9.5 in frost flowers, bulk ice cores, and brines from artificial sea ice grown at an outdoors
456 experimental facility. In the Arctic Ocean, pH_T ranged from 7.7 to 12.1 in frost flowers and sea
457 ice brines (Fransson et al., 2013), and from 8.3 to 8.5 (free proton scale, pH_F) in sackhole brines
458 ($S = 68 - 163$) (Miller et al., 2011a) in the Amundsen Gulf, while Rysgaard et al. (2012)
459 reported pH_T values between 9.9 and 10.1 in sea ice meltwater. In all these previous field
460 studies, the pH values at in situ (below-zero) temperatures have been computed from measured
461 TA and DIC in sea ice environments (Brown et al., 2014; Papadimitriou et al., 2009;
462 Papadimitriou et al., 2007) or from the pH measured directly in the sea ice medium at above-
463 zero temperatures and either TA or DIC (Brown et al., 2014; Delille et al., 2007; Fransson et
464 al., 2011; Gleitz et al., 1995; Hare et al., 2013; Miller et al., 2011a). In those instances, the pH
465 at in situ (below-zero) temperatures has been derived by solving the system of equations that
466 describe the thermodynamic relationships of the marine carbonate system (DOE, 1994) but
467 with the caveat that the relevant equilibrium constants have not yet been characterized at sub-
468 zero temperatures. Therefore, the use of this approach and the derived pH at the in situ (below-
469 zero) temperatures rely on extrapolation of the existing oceanographic salinity and temperature
470 functions of the equilibrium constants with discouragingly large uncertainties (Brown et al.,
471 2014).

472 The electrochemical characterization of the Tris buffer system in this study enables the
473 spectrophotometric characterization of pH indicator dyes in seawater-based hypersaline media
474 at below-zero temperatures. Both techniques and their results will free the sea ice
475 biogeochemical community from the uncertainty in the measurement of pH in sea ice by
476 affording investigators direct pH determination in sea ice brines down to -6°C and salinity 100.
477 Sea ice has been found to become impermeable at a porosity less than 5% (as relative brine
478 volume), coincident with a sea ice temperature of -5°C at a bulk sea ice salinity of 5 (Cox and
479 Weeks, 1975; Golden et al., 1998), or colder in more saline bulk sea ice, and vice versa, based
480 on the phase relationships in the medium (Cox and Weeks, 1983). Hence, sea ice in the current
481 experimental temperature range ($-2 \leq t \leq -6^{\circ}\text{C}$) is permeable to material transport via the brine
482 channels. As a result, the current experimental conditions are pertinent to the study of the
483 exchange potential of the brine carbonate system in sea ice with the underlying ocean and the
484 atmosphere above.

485 Major compositional changes in the internal brine in sea ice will occur at temperatures
486 well below -6°C as a result of extensive precipitation of hydrated salts, such as mirabilite,
487 gypsum, and hydrohalite (Butler et al., 2016; Butler and Kennedy, 2015; Marion, 2001).
488 Consequently, a different logistical approach is required for the study of the brine carbonate
489 system in the coldest compositional spectrum in sea ice, which is nearest to the atmosphere.
490 Further work below the minimum temperature presented here must take into account mineral
491 dynamics in sea ice for the determination of the chemical composition of the internal brines,
492 which will inform the composition of synthetic or natural solutions to be used in the laboratory
493 for the characterization of pH buffers and indicator dyes.

494

495 **Conclusions**

496 The current data set established explicitly the value of one of the important parameters
497 in the study of the carbonate system, the pH of the Tris-HCl buffer system, in sub-zero
498 temperature saline environments and within international standards. The pH of the Tris buffer
499 was fully characterized on the total proton scale in the temperature range from 25°C to the
500 freezing point of $S = 35$ seawater (freezing point: -1.93°C) and seawater-derived brines up to
501 a salinity of 100 (freezing point: -6.0°C). The difference between measurements at sub-zero
502 temperatures and the extrapolated values computed from the existing above-zero temperature
503 data sets may be negligible at $S = 35$ in terms of both the apparent standard potential of the
504 electrochemical Harned cell and the equimolal pH_{Tris} but increased systematically with
505 increasing salinity at all temperatures. Based on the apparent standard potential of the Harned

506 cell, this discrepancy was found to be equivalent to 0.118 pH unit at the highest salinity
507 investigated here ($S = 100$), a substantial deviation with consequent discrepancies in other
508 parameters of the carbonate system derived from it relying on extrapolation of existing
509 electrochemical and oceanographic data sets defined for above-zero temperatures and $S = 0 -$
510 50 . Hence, the current data will provide considerable improvement in the study of pH in cold
511 saline and hypersaline conditions relative to the only choice of extrapolation available until
512 now to biogeochemists. For a more complete characterization of the carbonate system in the
513 cryosphere, the dissociation constants of its weak acids and bases (e.g., carbonic and boric
514 acids) must be determined at below-zero temperatures.

515

516 **Acknowledgements**

517 We thank Makaila Lashomb for training S. Papadimitriou in the Harned cell protocol,
518 Britain Richardson for running the Harned cell at the highest salinities, Guy Emanuele for his
519 laboratory support, and George Anderson for providing the coulometric measurements and the
520 tickets for the La Jolla Symphony & Chorus concerts. We also thank two anonymous reviewers
521 for their helpful comments. The work was supported by NERC grant NE/J011096/1.

522 **References**

- 523 Arrigo, K.R., Worthen, D.L., Lizotte, M.P., Dixon, P., Dieckmann, G.S., 1997. Primary
524 production in Antarctic sea ice. *Science* 276, 394-397.
- 525 Assur, A., 1958. Composition of sea ice and its tensile strength in Arctic sea ice. U. S.
526 National Academy of Sciences, National Research Council, Publ 598, 106-138.
- 527 Bates, N.R., Mathis, J.T., 2009. The Arctic Ocean marine carbon cycle: evaluation of air-
528 sea CO₂ exchanges, ocean acidification impacts and potential feedbacks. *Biogeosciences*
529 6, 2433-2459.
- 530 Bates, N.R., Moran, S.B., Hansell, D.A., Mathis, J.T., 2006. An increasing CO₂ sink in the
531 Arctic Ocean due to sea-ice loss, *Geophys. Res. Lett.*, 33, 1-77, 2006.
- 532 Bates, R.G., Bower, V.E., 1954. Standard potential of the silver-silver-chloride electrode
533 from 0° to 95°C and the thermodynamic properties of dilute hydrochloric acid solutions.
534 *J. Res. Natl. Bur. Stand. (US)* 53, 283-290.
- 535 Bates, R.G., 1973. *Determination of pH: Theory and practice*, Wiley, New York.
- 536 Brown, K.A., Miller, L.A., Davelaar, M., Francois, R., Tortell, P.D., 2014. Over-
537 determination of the carbonate system in natural sea-ice brine and assessment of carbonic
538 acid dissociation constants under low temperature, high salinity conditions. *Mar. Chem.*
539 165, 36-45.
- 540 Butler, B.M., Kennedy, H., 2015. An investigation of mineral dynamics in frozen seawater
541 brines by direct measurement with synchrotron X-ray powder diffraction. *J. Geophys.*
542 *Res. Oceans* 120, 5686-5697, doi:10.1002/2015JC011032.
- 543 Butler, B.M., Papadimitriou, S., Santoro, A., Kennedy, H., 2016. Mirabilite solubility in
544 equilibrium sea ice brines. *Geochim. Cosmochim. Acta* 182, 40-54.
- 545 Campbell, D.M., Millero, F.J., Roy, R., Roy, L., Lawson, M., Vogel, K.M., Moore, C.P.,
546 1993. The standard potential for the hydrogen-silver, silver chloride electrode in
547 synthetic seawater. *Mar. Chem.* 44, 221-233.
- 548 Chierici, M., Fransson, A., 2009. Calcium carbonate saturation in the surface water of the
549 Arctic Ocean: undersaturation in freshwater influenced shelves. *Biogeosciences* 6, 2421-
550 2431.
- 551 Cox, G.F.N., Weeks, W.F., 1983. Equations for determining the gas and brine volumes in
552 sea ice samples. *J. Glaciol.* 29, 306-316.
- 553 Cox, G.F.N., Weeks W.F., 1975. Brine drainage and initial salt entrapment in sodium
554 chloride ice. CRREL Research Report 345.

555 Delille, B., Jourdain, B., Borges, A.V., Tison, J.-L., Delille, D., 2007. Biogas (CO₂, O₂,
556 dimethylsulfide) dynamics in spring Antarctic fast ice. *Limnol.Oceanogr.* 52, 1367-1379.

557 DelValls, T.A., Dickson, A.G., 1998. The pH of buffers based on 2-amino-2
558 hydroxymethyl-1,3-propanediol ('tris') in synthetic seawater. *Deep-Sea Res.* 45, 1541-
559 1554.

560 Deming, J.W., 2010. Sea ice bacteria and viruses, in: Thomas, D.N., Dieckmann, G.S.
561 (Eds.), *Sea Ice*, second ed. Wiley-Blackwell, Oxford, pp. 247-282.

562 Dickson, A.G., 1990a. The thermodynamics of the dissociation of boric acid in synthetic
563 seawater from 273.13 to 318.15 K. *Deep-Sea Res.* 37, 755-766.

564 Dickson, A.G., 1990b. Standard potential of the reaction: $\text{AgCl(s)} + \frac{1}{2}\text{H}_2(\text{g}) = \text{Ag(s)} +$
565 HCl(aq) , and the standard acidity constant of the ion HSO_4^- in synthetic sea water from
566 273.15 to 318.15 K. *J. Chem. Thermodyn.* 22, 113-127.

567 Dieckmann, G.S., Nehrke, G., Uhlig, C., Göttlicher, J., Gerland, S., Granskog, M.A.,
568 Thomas, D.N., 2010. Brief communication: Ikaite (CaCO₃·6H₂O) discovered in Arctic
569 sea ice. *The Cryosphere* 4, 227-230.

570 Dieckmann, G.S., Nehrke, G., Papadimitriou, S., Göttlicher, J., Steininger, R., Kennedy, H.,
571 Wolf-Gladrow, D., Thomas, D.N., 2008. Calcium carbonate as ikaite crystals in Antarctic
572 sea ice. *Geophys. Res. Lett.* 35, L08501, doi: 10.1029/2008gl033540.

573 DOE, 1994. Handbook of methods for the analysis of the various parameters of the carbon
574 dioxide system in sea water; version 2, Dickson, A.G., Goyet, C. (Eds.), ORNL/CDIAC-
575 74.

576 Fischer, M., Thomas, D.N., Krell, A., Nehrke, G., Göttlicher, J., Norman, L., Meiners, K.M.,
577 Riaux-Gobin, C., Dieckmann, G.S., 2013. Quantification of ikaite in Antarctic sea ice.
578 *Antarct. Sci.* 25, 421-432.

579 Fransson, A., Chierici, M., Miller, L.A., Carnat, G., Shadnick, E., Thomas, H., Pineault, S.,
580 Papakyriakou, T.N., 2013. Impact of sea-ice processes on the carbonate system and ocean
581 acidification at the ice-water interface of the Amundsen Gulf, Arctic Ocean. *J. Geophys.*
582 *Res.* 118, 7001-7023.

583 Gleitz, M., v.d. Loeff, M.R., Thomas, D.N., Dieckmann, G.S., Millero, F.J., 1995.
584 Comparison of summer and winter inorganic carbon, oxygen and nutrient concentrations
585 in Antarctic sea ice brine. *Mar. Chem.* 51, 81-91.

586 Golden, K.M., Ackley, S.F., Lytle, V.I., 1998. The percolation phase transition in sea ice.
587 *Science* 282, 2238-2241.

588 Hales, B., Chipman, D., Takahashi, T., 2004. High-frequency measurements of partial
589 pressure and total concentration of carbon dioxide in seawater using microporous
590 hydrophobic membrane contactors. *Limnol. Oceanogr. Methods* 2, 356-364.

591 Hare, A.A., Wang, F., Barber, D., Geilfus, N.X., Galley, R.J., Rysgaard, S., 2013. pH
592 evolution in sea ice grown at an outdoor experimental facility. *Mar. Chem.* 154, 46-54.

593 IUPAC, 2002. Measurement of pH. Definition, standards, and procedures (IUPAC
594 recommendations 2002). *Pure Appl. Chem.* 74, 2169-2200.

595 Khoo, K.H., Ramette, R.W., Culberson, C.H., Bates, R.G., 1977. Determination of hydrogen
596 ion concentrations in seawater from 5 to 40°C: Standard potential at salinities from 20 to
597 40‰. *Anal. Chem.* 49, 29-34.

598 Liu, X., Patsavas, M.C., Byrne, R.H., 2011. Purification and characterization of meta-Cresol
599 Purple for spectrophotometric seawater pH measurements. *Environ. Sci. Technol.* 45,
600 4862-4868.

601 Marion, G.M., 2001. Carbonate mineral solubility at low temperatures in the Na-K-Mg-Ca-
602 H-Cl-SO₄-OH-HCO₃-CO₃-CO₂-H₂O system. *Geochim. Cosmochim. Acta* 65, 1883–
603 1896.

604 Miller, L.A., Fripiat, F., Else, B.G.T., Bowman, J.S., Brown, K.A., Collins, R.E., Ewert, M.,
605 Fransson, A., Gosselin, M., Lannuzel, D., Meiners, K.M., Michel, C., Nishioka, J.,
606 Nomura D., Papadimitriou S., Russell L.M., Sørensen L.L., Thomas D.N., Tison J.-L.,
607 van Leeuwe, M.A., Vancoppenolle, M., Wolff, E.W., Zhou, J., 2015. Methods for
608 biogeochemical studies of sea ice: The state of the art, caveats, and recommendations.
609 *Elementa: Science of the Anthropocene* 3, 000038, doi:
610 10.12952/journal.elementa.000038.

611 Miller, L.A., Carnat, G., Else, B.G.T., Sutherland, N., Papakyriakou, T.N., 2011a.
612 Carbonate system evolution at the Arctic Ocean surface during autumn freeze-up. *J.*
613 *Geophys. Res.* 116, C00G04, doi: 10.1029/2011JC007143.

614 Miller, L.A., Papakyriakou, T.N., Collins, R.E., Deming, J.W., Ehn, J.K., Macdonald, R.W.,
615 Mucci, A., Owens, O., Raudsepp, M., Sutherland, N., 2011b. Carbon dynamics in sea
616 ice: A winter flux time series. *J. Geophys. Res.* 116, C02028, doi:
617 10.1029/2009JC006058.

618 Millero, F.J., 2009. Use of the Pitzer equations to examine the dissociation of TRIS in NaCl
619 solutions. *J. Chem. Eng. Data* 54, 342-344.

620 Millero, F.J., DiTrolino, B., Suarez, A.F., Lando, G., 2009. Spectroscopic measurements of
621 the pH in NaCl brines. *Geochim. Cosmochim. Acta* 73, 3109-3114.

622 Millero, F.J., Graham, T.B., Huang, F., Bustos-Serrano, H., Pierrot, D., 2006. Dissociation
623 constants of carbonic acid in seawater as a function of salinity and temperature. *Mar.*
624 *Chem.* 100, 80-94.

625 Millero, F.J., Pierrot, D., Lee, K., Wanninkhof, R., Feely, R., Sabine, C.L., Key, R.M.,
626 Takahashi, T., 2002. Dissociation constants for carbonic acid determined from field
627 measurements. *Deep-Sea Res. Part I* 49, 1705-1723.

628 Millero, F.J., Zhang, J.Z., Fiol, S., Sotolongo, S., Roy, R.N., Lee K., Mane S., 1993. The
629 use of buffers to measure the pH of seawater. *Mar. Chem.* 44, 143-152.

630 Munro, D.R., Dunbar, R.B., Mucciarone, D.A., Arrigo, K.R., Long, M.C., 2010. Stable
631 isotopic composition of dissolved inorganic carbon and particulate organic carbon in sea
632 ice from the Ross Sea, Antarctica. *J. Geophys. Res.* 115, C09005,
633 doi:10.1029/2009JC005661.

634 Notz, D., Worster, M.G., 2009. Desalination processes in sea ice revisited. *J. Geophys. Res.*
635 114, C05006. doi: 10.1029/2008JC004885.

636 Papadimitriou, S., Kennedy, H., Kennedy, P., Thomas, D.N., 2014. Kinetics of ikaite
637 precipitation and dissolution in seawater-derived brines at subzero temperatures to 265
638 K. *Geochim. Cosmochim. Acta* 140, 199-211, doi: 10.1016/j.gca.2014.05.031.

639 Papadimitriou, S., Kennedy, H., Kennedy, P., Thomas, D.N., 2013. Ikaite solubility in
640 seawater-derived brines at 1 atm and sub-zero temperatures to 265 K. *Geochim.*
641 *Cosmochim. Acta* 109, 241-253, doi:10.1016/j.gca.2013.01.044.

642 Papadimitriou, S., Kennedy, H., Norman, L., Kennedy, D.P., Thomas, D.N., 2012. The
643 effect of biological activity, CaCO₃ mineral dynamics, and CO₂ degassing in the
644 inorganic carbon cycle in sea ice in late winter-early spring in the Weddell Sea,
645 Antarctica. *J. Geophys. Res.* 117, C08011, doi: 10.1029/2012JC008058.

646 Papadimitriou, S., Kennedy, H., Kattner, G., Dieckmann, G.S., Thomas, D.N., 2004.
647 Experimental evidence for carbonate precipitation and CO₂ degassing during sea ice
648 formation. *Geochim. Cosmochim. Acta* 68, 1749-1761.

649 Papadimitriou, S., Thomas, D.N., Kennedy, H., Kuosa, H., Dieckmann, G.S., 2009.
650 Inorganic carbon removal and isotopic enrichment in Antarctic sea ice gap layers during
651 early austral summer. *Mar. Ecol. Prog. Ser.* 386, 15-27.

652 Papadimitriou, S., Thomas, D.N., Kennedy, H., Haas, C., Kuosa, H., Krell, A., Dieckmann,
653 G.S., 2007. Biogeochemical composition of natural sea ice brines from the Weddell Sea
654 during early austral summer. *Limnol. Oceanogr.* 52, 1809-1823.

655 Pitzer, K.S., 1973. Thermodynamics of electrolytes. I. Theoretical basis and general
656 equations. *J. Phys. Chem.* 77, 268-277.

657 Pratt, K.W., 2014. Measurement of pH_T values of Tris buffers in artificial seawater at
658 varying mole ratios of Tris:Tris-HCl. *Mar. Chem.* 162, 89-95.

659 Robert-Baldo, G.L., Morris, M.J., Byrne, R.H., 1985. Spectrophotometric determination of
660 seawater pH using Phenol Red. *Anal. Chem.* 57, 2564-2567.

661 Rysgaard, S., Bendtsen, J., Delille, B., Dieckmann, G.S., Glud, R.N., Kennedy, H.,
662 Mortensen, J., Papadimitriou, S., Thomas, D.N., Tison, J.-L., 2011. Sea ice contribution
663 to the air–sea CO₂ exchange in the Arctic and Southern Oceans. *Tellus B* 63, 823-830.

664 Rysgaard, S., Glud, R.N., Lennert, K., Cooper, M., Halden, N., Leakey, R.J.G., Hawthorne,
665 F.G., Barber, D., 2012. Ikaite crystals in melting sea ice – implications for pCO₂ and pH
666 levels in Arctic surface waters. *The Cryosphere Discussions* 6, 1015-1035,
667 doi:10.5194/tcd-6-1015-2012.

668 Rysgaard, S., Glud, R.N., Sejr, M.K., Bendtsen, J., Christensen, P.B., 2007. Inorganic
669 carbon transport during sea ice growth and decay: A carbon pump in polar seas. *J.*
670 *Geophys. Res. Oceans* 112, C03016, doi: 10.1029/2006JC003572.

671 Rysgaard, S., Sogaard, D.H., Cooper, M., Pucko, M., Lennert, K., Papakyriakou, T.N.,
672 Wang, F., Geilfus, N.X., Glud, R.N., Ehn, J., McGinnis, D.F., Attard, K., Sievers, J.,
673 Deming, J.W., Barber, D., 2013. Ikaite crystal distribution in winter sea ice and
674 implications for CO₂ system dynamics. *The Cryosphere* 7, 707-718.

675 Takahashi, T., Sutherland, S.C., Sweeney, C., Poisson, A., Metzl, N., Tilbrook, B., Bates,
676 N., Wanninkhof, R., Feely, R.A., Sabine, C., Olafsson, J., Nojiri, Y., 2002. Global sea-
677 air CO₂ flux based on climatological surface ocean pCO₂, and seasonal biological and
678 temperature effects. *Deep–Sea Res. Part II* 49, 1601-1622.

679 UNESCO, 1983. Algorithms for computation of fundamental properties of seawater.
680 *Unesco Technical Papers in Marine Science* 44, 53 pp.

681 Wren, S.V., Donaldson, D.J., 2012. Laboratory study of pH at the air-ice interface. *J. Phys.*
682 *Chem. C* 116, 10171-10180.

683 Yamamoto-Kawai, M., McLaughlin, F.A., Carmack, E.C., 2011. Effects of ocean
684 acidification, warming and melting of sea ice on aragonite saturation of the Canada Basin
685 surface water. *Geophys. Res. Lett.* 38, L03601, doi: 10.1029/2010gl045501.

686 Yamamoto-Kawai, M., McLaughlin, F.A., Carmack, E.C., Nishino, S., Shimada, K., 2009.
687 Aragonite undersaturation in the Arctic Ocean: Effects of ocean acidification and sea ice
688 melt. *Science* 326, 1098-1100.

690 **Table 1.** The composition and ionic strength (I) of synthetic seawater of nominal salinity 35^a.

Component	mol kg _{H₂O} ⁻¹	mol kg _{solution} ⁻¹
NaCl	0.42762 - m_1	0.41262
Na ₂ SO ₄	0.02927	0.02824
KCl	0.01058	0.01021
MgCl ₂	0.05474	0.05282
CaCl ₂	0.01075	0.01037
HCl	m_1	0
^b Tris	m_2	0
Cl ⁻	0.5692	0.5492
I	0.7225	

691 ^aThe molality (m_s , in mol kg_{H₂O}⁻¹) of the salts in synthetic brines of salinity $S > 35$ and ionic
692 strength I_s was calculated as $m_s = m_{35} I_s / I_{35}$, with $I_s = 19.9184 S / (1000 - 1.00198 S)$ (DeIValles
693 and Dickson, 1998). The concentration in mol kg_{solution}⁻¹ was calculated by computing the total
694 salt mass ($\sum \text{mass}_{\text{salt}}$) and multiplying each salt molality with the factor, $1000 / (1000 +$
695 $\sum \text{mass}_{\text{salt}})$.

696 ^bThe molalities of HCl and Tris were chosen independent of ionic strength. In cells (B) and
697 (C), $m_2 = 0$; in cells (D) and (E), $m_2 = 2m_1$ for equimolar Tris buffers.

698

699

700 **Table 2.** The apparent standard potential (E_o^*) and its regression standard error ($\sigma_{E_o^*}$) (both in
701 V) of cells (B) and (C). Values in *italics* were derived from the salinity and temperature
702 extrapolation of equations (15) and (16) in Dickson (1990b) and equations (17) and (18) with
703 the coefficients derived from the combined data sets in Campbell et al. (1993).

T	S	this study		Dickson (1990b)	Campbell et al. (1993)
		E_o^*	$\sigma_{E_o^*}$	E_o^*	E_o^*
25.0	35	0.24642	0.00005	0.24628	0.24630
0.0		0.25477	0.00004	0.25468	0.25474
-0.6		0.25496	0.00005	<i>0.25485</i>	<i>0.25439</i>
-1.2		0.25516	0.00006	<i>0.25502</i>	<i>0.25458</i>
-1.7		0.25535	0.00006	<i>0.25518</i>	<i>0.25475</i>
25.0	45	0.24680	0.00003	0.24651	0.24655
0.0		0.25466	0.00004	0.25442	0.25448
-2.5		0.25540	0.00004	<i>0.25515</i>	<i>0.25470</i>
25.0	50	0.24664	0.00008	<i>0.24641</i>	<i>0.24582</i>
0.0		0.25428	0.00009	<i>0.25411</i>	<i>0.25358</i>
-2.8		0.25511	0.00009	<i>0.25491</i>	<i>0.25447</i>
25.0	60	0.24637	0.00006	<i>0.24579</i>	<i>0.24516</i>
0.0		0.25363	0.00006	<i>0.25314</i>	<i>0.25259</i>
-3.4		0.25461	0.00006	<i>0.25405</i>	<i>0.25364</i>
25.0	70	0.24578	0.00002	<i>0.24462</i>	<i>0.24399</i>
0.0		0.25277	0.00008	<i>0.25166</i>	<i>0.25114</i>
-4.0		0.25391	0.00009	<i>0.25268</i>	<i>0.25235</i>
25.0	85	0.24519	0.00013	<i>0.24180</i>	<i>0.24122</i>
0.0		0.25177	0.00004	<i>0.24846</i>	<i>0.24805</i>
-5.0		0.25311	0.00004	<i>0.24962</i>	<i>0.24949</i>
25.0	100	0.24381	0.00012	<i>0.23756</i>	<i>0.23713</i>
0.0		0.24989	0.00006	<i>0.24388</i>	<i>0.24368</i>
-6.0		0.25142	0.00006	<i>0.24515</i>	<i>0.24536</i>

704

705

706 **Table 3.** The potential (E_{Tris} , in V) of cells (D) and (E) with Tris buffer solutions in synthetic seawater and brines. The E_{Tris} is the value after
707 adjustment by $\Delta E_{\text{o}}^{\text{BB}}$ (in V) so that the standard potential of the cells corresponds to that of Bates and Bower (1954) [see *Methods* and DelValls
708 and Dickson (1998) for details]. The concentrations of the Tris species (m_{Tris} , $m_{\text{Tris-H}^+}$) and total chloride (m_{Cl^-}) in solution are in mol $\text{kg}_{\text{H}_2\text{O}}^{-1}$,
709 while the pH_{Tris} is the negative common logarithm of the proton concentration in mol $\text{kg}_{\text{solution}}^{-1}$ on the total proton scale.

S	t (°C)	m_{Tris}	$m_{\text{Tris-H}^+}$	m_{Cl^-}	$\Delta E_{\text{o}}^{\text{BB}}$	E_{Tris}			pH_{Tris}		
35	24.996	0.04	0.04	0.56918	-0.00012	0.73863	0.73873	0.73870	8.092	8.094	8.093
	0.004					0.75129	0.75136	0.75134	8.933	8.934	8.934
	-0.001					0.75130	0.75137	0.75134	8.933	8.934	8.934
	-0.619					0.75158	0.75164	0.75163	8.955	8.957	8.956
	-1.165					0.75170	0.75190	0.75187	8.972	8.976	8.975
	-1.712					0.75205	0.75216	0.75214	8.994	8.996	8.996
45	25.000			0.73949	0.00000	0.73317	0.73320		8.111	8.112	
	-0.003					0.74633	0.74628		8.962	8.961	
	-2.499					0.74755	0.74751		9.054	9.054	
50	24.996			0.82602	0.00000	0.73080	0.73080		8.125	8.125	
	-0.002					0.74421	0.74418		8.980	8.980	
	-2.795					0.74561	0.74558		9.084	9.084	
60	24.997			1.00190	0.00000	0.72655	0.72659		8.146	8.147	
	-0.006					0.74024	0.74037		9.008	9.010	
	-3.422					0.74202	0.74215		9.137	9.139	
70	24.998			1.18141	0.00000	0.72280	0.72284		8.169	8.170	
	-0.002					0.73690	0.73693		9.038	9.039	
	-3.999					0.73904	0.73908		9.190	9.191	
35	0.003	0.02	0.04	0.56918	+0.00002	0.73511	0.73505	0.73506	8.634	8.633	8.633
45	0.002					0.73019	0.73013	0.73012	8.664	8.663	8.663
50	24.996					0.82599	0.00000	0.71299	0.71300		7.824
	-0.002					0.72782	0.72779		8.678	8.677	
	-2.795					0.72939	0.72937		8.782	8.781	

710 **Table 3** (continued)

S	t (°C)	m _{Tris}	m _{Tris-H⁺}	m _{Cl⁻}	ΔE_o^{BB}	E _{Tris}			pH _{Tris}		
60	24.997	0.02	0.04	1.00163	0.00000	0.70879	0.70876		7.846	7.845	
	-0.006					0.72399	0.72402		8.708	8.708	
	-3.422					0.72598	0.72600		8.837	8.837	
70	24.998			1.18130	0.00000	0.70504	0.70504		7.869	7.869	
	-0.002					0.72053	0.72052		8.736	8.736	
	-3.999					0.72291	0.72290		8.888	8.888	
85	24.996			1.45800	+0.00002	0.70046	0.70046	0.70043	7.900	7.900	7.900
	24.999					0.70049	0.70024	0.70025	7.901	7.897	7.897
	0.000					0.71642			8.778		
	-0.001					0.71660	0.71650	0.71650	8.781	8.779	8.779
	-5.001					0.71950			8.970		
	-5.000					0.71968	0.71960	0.71961	8.974	8.972	8.972
100	25.000			1.74393	+0.00002	0.69605	0.69573	0.69567	7.935	7.929	7.928
	0.001					0.71264	0.71261	0.71261	8.828	8.827	8.827
	-6.001					0.71643	0.71643	0.71641	9.063	9.063	9.062

711

712

List of Figure Captions

Figure 1. The value of $E' = E + k \ln(m_{\text{HCl}} m_{\text{Cl}^-})$ versus m_{HCl} in synthetic seawater ($S = 35$) in panels (a) and (b), and in $S = 45$ synthetic seawater-based brine in panels (c) and (d). Data from previous studies are from Khoo et al. (1997) (\diamond), Dickson (1990b) (\circ), and Campbell et al. (1993) (\square). The solid lines in all panels show the quadratic fit in m_{HCl} to the E' values for the determination of E_o^* as the intercept at $m_{\text{HCl}} = 0$.

Figure 2. The apparent standard potential of the Harned cell with synthetic seawater and synthetic seawater-based brine as a function of salinity in panels (a) and (b), and as a function of temperature in panel (c). Open circles represent experimental data from Dickson (1990b). The solid line represents the best-fit equation (16) of Dickson (1990b) within its experimental ionic strength and temperature ranges, while the dashed line represents its extrapolation to $S > 45$ and below-zero temperatures. In panel (c), the temperatures below the freezing point of $S = 35$ seawater (-1.93°C ; dotted vertical line) represent the freezing points at $S > 35$ salinities.

Figure 3. Residuals in E_o^* as a function of (a) temperature and (b) ionic strength (molal). The residuals are between the experimental values and the fitted values from equation (3). The experimental values are from Table 2 in this study (+), from Table 3 in Dickson (1990b) (\circ), and from Table 3 in Campbell et al. (1993) (\square).

Figure 4: The pH of Tris buffer solutions (on the total proton scale) in synthetic seawater and synthetic brine as a function of salinity in panels (a) and (b), and as a function of temperature at sub-zero temperatures in panel (c). The observations from this study are from the equimolar Tris buffer (+) (molality ratio, $R_{\text{Tris}} = m_{\text{Tris}}/m_{\text{Tris-H}^+} = 1$) and the non-equimolar Tris buffer (\circ) ($R_{\text{Tris}} = 0.5$). The solid line represents the best-fit equation (18) of DelValls and Dickson (1998) within its experimental salinity and temperature ranges, while the dashed line represents its extrapolation to $S < 20$ and $S > 40$, and below-zero temperatures. In panel (c), the temperatures below the freezing point of $S = 35$ seawater (-1.93°C ; dotted vertical line) represent the freezing points at $S > 35$ salinities.

Figure 5. Residuals in pH_{Tris} (in $\text{mol kg}_{\text{solution}}^{-1}$ on the total proton scale) as a function of temperature in panels (a) and (b), and as a function of salinity in panels (c) and (d). The residuals are between the experimental values and the fitted values from equation (7) for the equimolar Tris buffer (molality ratio, $R_{\text{Tris}} = m_{\text{Tris}}/m_{\text{Tris-H}^+} = 1$) in panels (a) and (c), and between the experimental values and the fitted values from equation (8) for the non-equimolar

Tris buffer ($R_{\text{Tris}} = 0.5$) in panels (b) and (d). The experimental values are from Table 3 in this study (+) and as computed from the results in Table 2 of DeValls and Dickson (1998) (\circ).

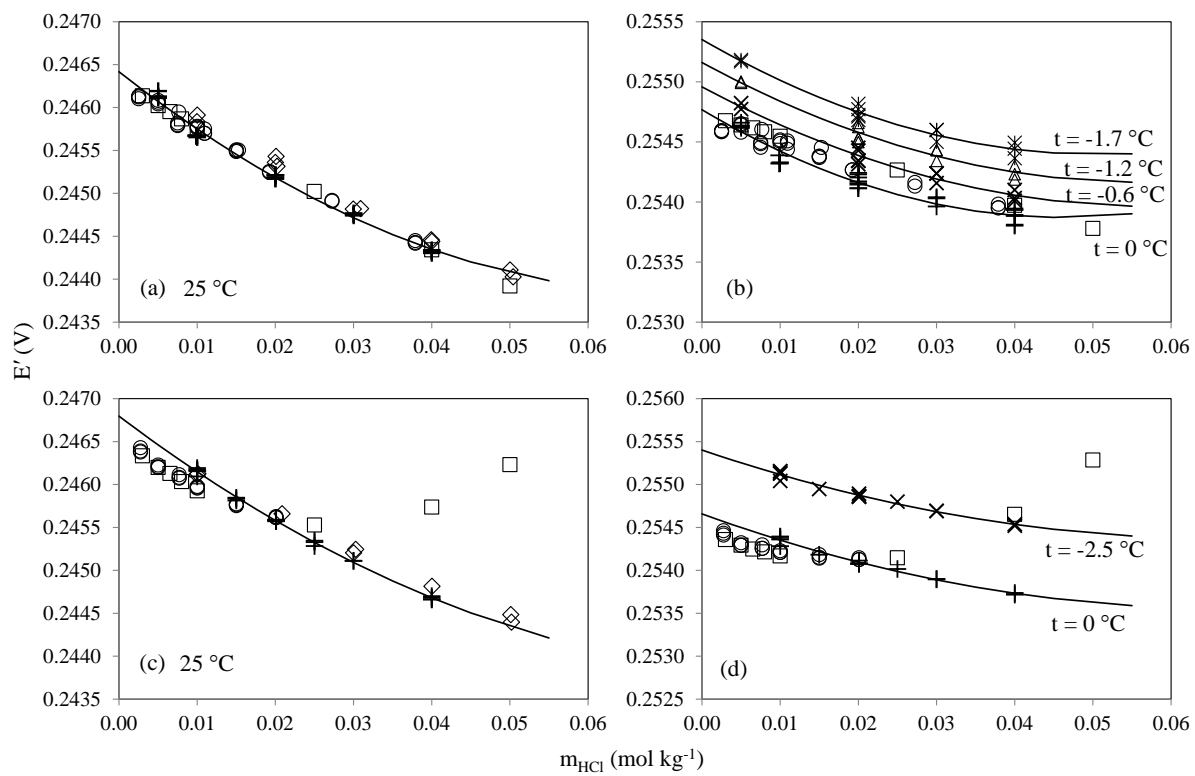


Figure 1

MARCHE_D1600001 Revised

Papadimitriou et al.

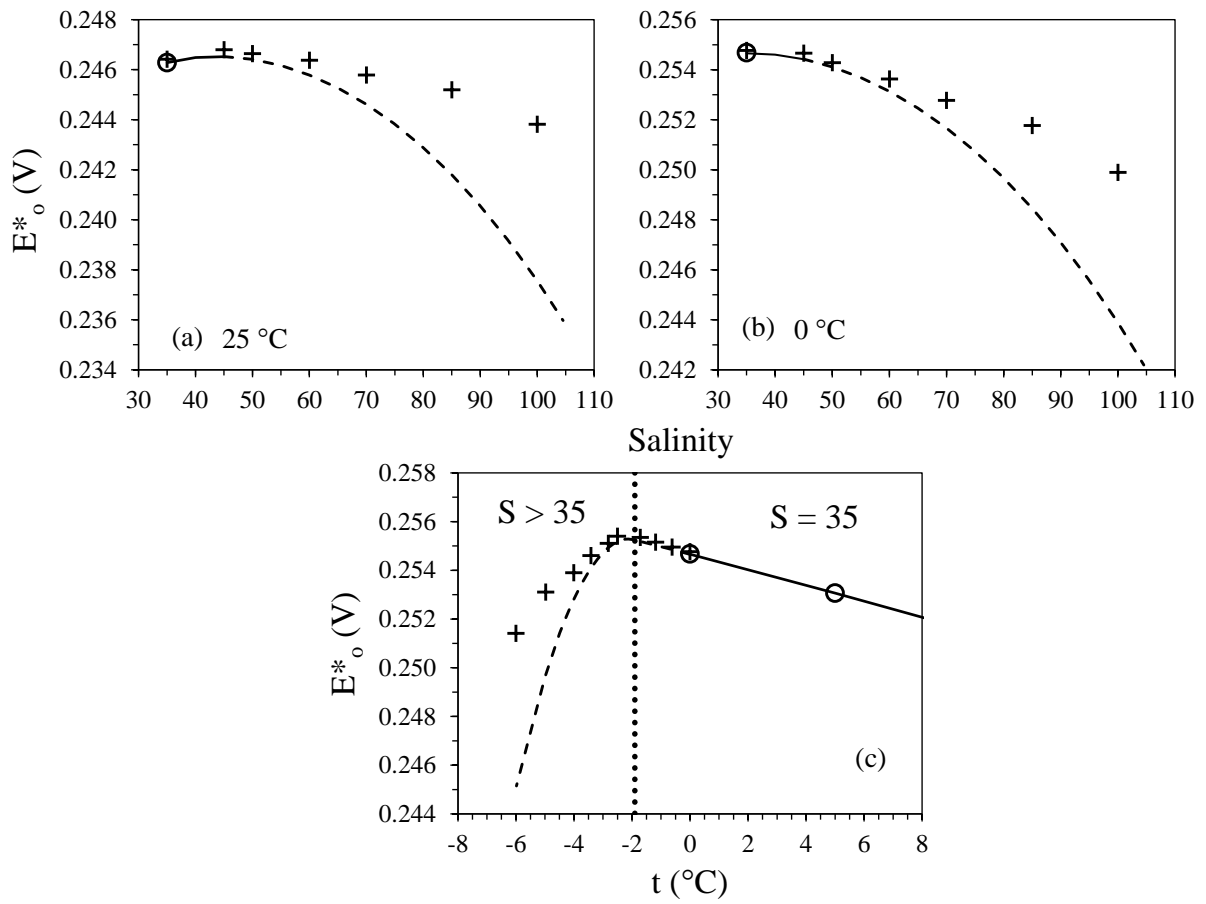


Figure 2

MARCHE_D1600001 Revised

Papadimitriou et al.

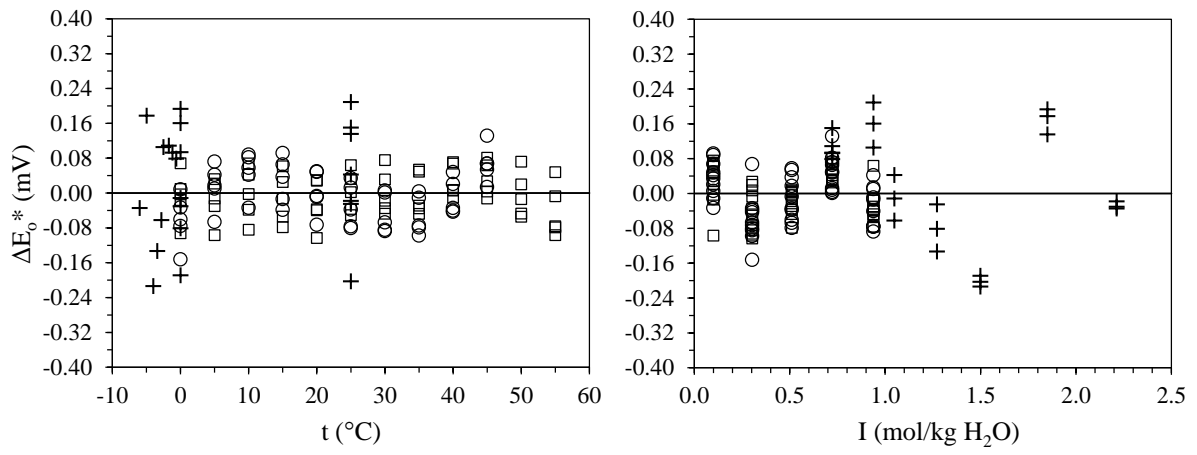


Figure 3

MARCHE_D1600001 Revised

Papadimitriou et al.

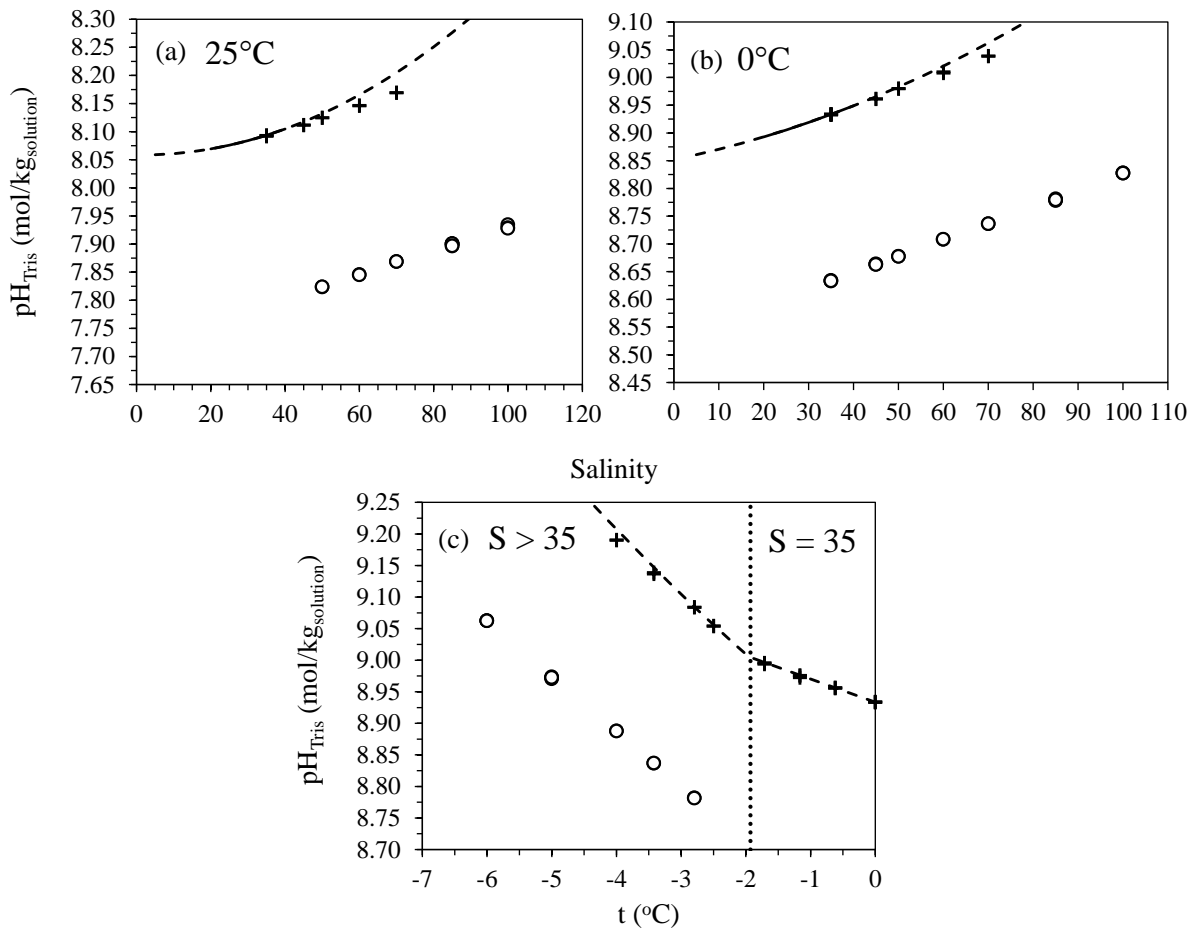


Figure 4

MARCHE_D1600001 Revised

Papadimitriou et al.

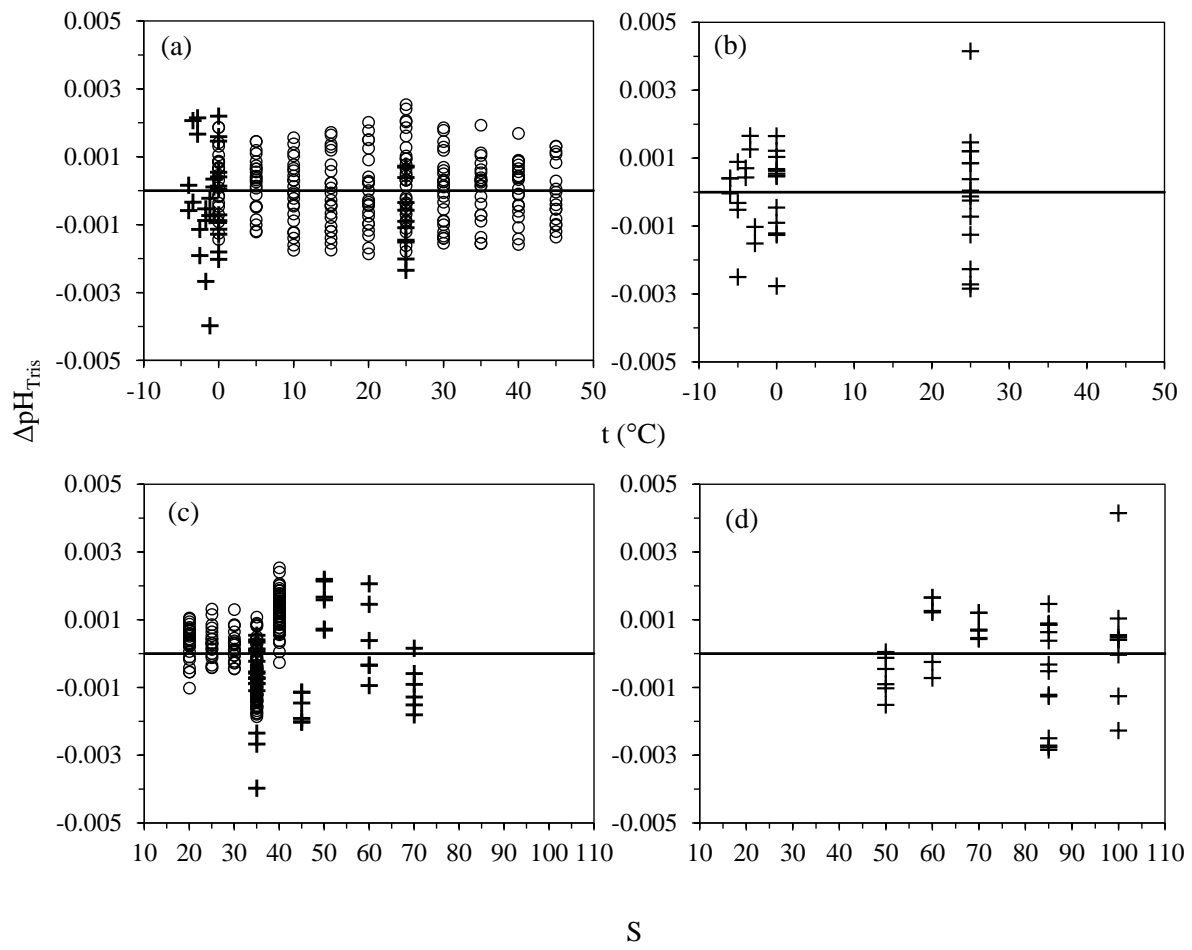


Figure 5

MARCHE_D1600001 Revised

Papadimitriou et al.